Combined Matrix-Isolation Infrared and Theoretical DFT and ab Initio Study of the Nonionized Valine Conformers

S. G. Stepanian,[†,‡] I. D. Reva,[‡] E. D. Radchenko,[‡] and L. Adamowicz*[,†]

Department of Chemistry, University of Arizona, Tucson, Arizona 85721, and Institute for Low-Temperature Physics and Engineering, National Academy of Sciences of Ukraine, 47 Lenin Avenue, Kharkov 310164, Ukraine

Received: November 17, 1998; In Final Form: March 30, 1999

We present results of the first experimental observation of the nonionized natural amino acid valine. The study has employed the matrix-isolation IR spectroscopy and the density functional theory (DFT) and ab initio calculations. In the calculations geometries of nine low-energy valine conformers were optimized using the DFT method with the B3LYP parametrization and the 6-31++G** basis set. Additionally, the relative energies of the conformers were calculated at the MP2/6-31++G** level. The harmonic frequencies and IR intensities were calculated for all the minima found. These data were used to separate and assign the bands of the valine conformers in the experimental spectra. We found that two valine conformers are present in the Ar matrix: one with a bifurcated $NH_2\cdots O{=}C$ H-bond (conformer **Ia**) and one with a $N\cdots H-O$ H-bond (conformer **IIa**). A trace amount of a third valine conformer with $NH_2\cdots O-C$ H-bond (conformer **IIIb**) was also detected. The conformational composition of the matrix-deposited nonionized valine was determined on the basis of observed and predicted IR intensities of the bands of different conformers. The composition is ∼94% of conformer **Ia**, ∼5% of conformer **IIa**, and less than 2% of conformer **IIIb**. The presence of three valine conformers in the Ar matrix results in broadening and/or in multiplex structures of some bands in the valine IR spectrum. Common features in the IR spectra of some nonionized natural aliphatic amino acids are discussed.

1. Introduction

Low thermal stability of natural amino acids creates significant problems in their investigations in the gas phase. Till now only the molecular structures of the simplest amino acids, glycine, α-alanine, and proline, have been studied experimentally in gas-phase samples.[1−14] These experimental investigations have demonstrated that glycine and alanine exist in the gas phase in the nonionized forms which correspond to the amino acid units present in peptides. This explains the interest in the nonionized amino acids and has motivated the present investigation.

Recently we demonstrated that the matrix-isolation IR spectroscopy combined with the DFT and ab initio calculations is a suitable tool to investigate the conformational behavior of amino acids.[8,13] The matrix-isolation method allows separation of the matrix deposition process, which may be very long in the case of a compound with a low vapor pressure, from the registration of the IR spectrum. Application of the low-temperature matrix-isolation technique to study structures of the nonionized glycine and α-alanine isolated in solid argon lead to identification of three low energy conformers of glycine[8] and two conformers of α-alanine.[13] All the structures found are stabilized by intramolecular H-bonding. The feature of the matrix-isolation IR method, which enables assignment of structurally similar conformers, is its high sensitivity to the intramolecular H-bonding. Moreover, the inert matrix environment hinders the rotation of the deposited molecules and eliminates rotational bands from the spectrum, thus simplifying its analysis in comparison to gaseous spectra where the rotational structure is present. A drawback of the IR matrix-isolation study is the presence of the interaction between the matrix material with the molecules of the studied system, which can lead to band shifts and splittings.

In our study on glycine, we examined the performance of the DFT and second-order many-body perturbation theory (MBPT = MP2) methods in predicting the vibrational frequencies and intensities of different conformers of this system.[8] We found that the DFT method with the B3LYP parametrization is capable of predicting the spectral characteristics in excellent agreement with the experimental data. The DFT results appeared to be even more accurate than the MP2 results. We also showed that inclusion of diffuse orbitals in the basis set significantly increases the accuracy of the calculated IR spectra. Subsequently we used the DFT/B3LYP method to analyze the IR matrix-isolation spectra of α-alanine.[13] Again we found an excellent agreement between the calculated and observed IR frequencies. In the present work we continue the study on conformational behavior of the natural amino acids and consider the matrix-isolated α-valine.

A multiple-minima potential energy surface is an inherent feature of the amino acid structural behavior. For example, the theoretical calculations predicted as many as eight minima for glycine[15−19] and 13 minima for alanine.[20,21] For larger amino acids the number of possible conformers increases significantly. Gronert and O'Hair located 42 conformers for cysteine and 51 conformers for serine.[22] It is obvious that the number of possible valine conformers is also large and it may create a problem in

* To whom correspondence should be addressed.
† Department of Chemistry.
‡ Institute for Low-Temperature Physics and Engineering.

10.1021/jp984457v CCC: $18.00
Published on Web 05/11/1999

an experimental investigation of the valine conformational composition.

The aim of the calculations performed in this work has been not to locate all possible valine conformers but only the lowest energy ones, which can be present in low-temperature inert matrixes. Similarities between the glycine and valine structures provide leads that allow location of the lowest energy points on the valine potential energy surface. The previous theoretical calculations of the glycine structure resulted in identification of eight conformers which differ in the relative position of the amino and carboxyl groups.[15−19] The calculated relative energies of the glycine conformers showed that among the eight conformers three species are the most stable. These are the conformer with a bifurcated $NH_2\cdots O{=}C$ H bond (conformer **I**), the conformer with a N···H−O H-bond (conformer **II**), and the conformer with a bifurcated $NH_2\cdots O-C$ H-bond (conformer **III**). These results are in full agreement with the experiment where the three glycine conformers (**I**−**III**) were detected. For α-alanine the analysis of the experimental data revealed presence of two conformers (**I** and **II**). Therefore we assumed that also in the case of valine the most stable conformers are those with intramolecular H-bonds (similar to conformers **I**−**III**). This assumption is in agreement with the results of the HF/4-21G calculations performed by Schäfer et al.[23] and with the recent results of the HF/6-31G* calculations of Shirazian and Gronert.[24]

2. Experimental Details

The IR spectra were registered with the updated SPECORD IR 75 spectrometer in the range 4000−400 cm^{-1}. The resolution in the range 4000−2500 cm^{-1} was 3 cm^{-1} and in the range 2500−400 cm^{-1} was 1 cm^{-1}. The spectrometer was sealed and blown through with dry nitrogen during the experiment to exclude any influence of the atmospheric H_2O and CO_2. The fill-up helium cryostat used in the matrix-isolation IR experiments was described elsewhere.[25]

The measurements were carried out for the commercially available α-valine. The matrix samples were prepared by a simultaneous deposition of the substance and the matrix gas onto a cooled CsI substrate. The matrix gas was 99.99% Ar. The substrate temperature was 14 K during matrix preparation. The compound studied was evaporated from the Knudsen cell at 152 °C. This temperature was found to be high enough to yield samples with sufficient concentration of the compounds but still sufficiently low to prevent its decomposition. The low-temperature quartz microbalance was used to measure the gaseous flows of the compound studied and of the matrix gas. By adjusting these flows we were able to prevent an appearance of autoassociates in the spectrum. This was accomplished at the relative concentration of valine to argon in the matrix equal to 1:1000.

The IR spectra of valine recorded immediately after sample deposition are presented in Figures 1 and 2. They show no bands of any valine decomposition products. Only a few weak bands corresponding to trace amounts of CO_2 and H_2O appear in the spectra, which are most probably due to CO_2 and H_2O absorbed on the surface of the solid compound used in the experiment.

3. Theoretical Methods

Since the Hartree−Fock (HF) method failed to predict the relative energies of the nonionized amino acid conformers correctly,[17,18] in the present study we have used the DFT and MP2[26,27] methods for the relative stability calculations. Also the DFT method was used for the harmonic frequency calculations. The DFT calculations were carried out with the three-

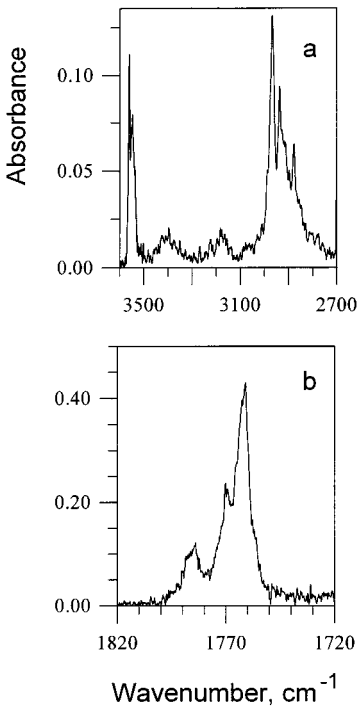

Figure 1. O−H stretching (a) and C═O stretching (b) vibration regions of the IR spectrum of valine. The spectrum is recordered for sample deposited at 14 K. The sample-to-matrix ratio is 1:1000.

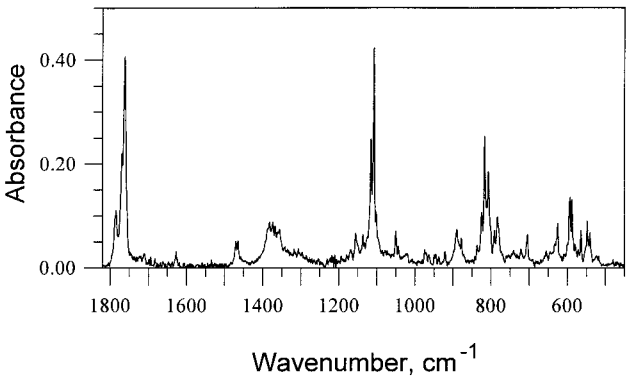

Figure 2. Fingerprint region of the IR spectrum of valine.

parameter density functional, usually abbreviated as B3LYP, which includes Becke's gradient exchange correction,[28] the Lee, Yang, Parr correlation functional,[29] and the Vosko, Wilk, and Nusair correlation functional.[30] The standard 6-31++G** basis set was used in the calculations.

In locating the most stable valine conformers we used the following strategy. First, for the three configurations of the amino acid fragment similar to glycine conformers **I**−**III** we identified all possible minima corresponding to rotation of the aliphatic side chain of valine around the $C_\alpha-C_6$ bond. In these calculations performed at the DFT/B3LYP/6-31G* level of theory we incrementally increased the rotation angle by 30° while all other geometrical parameters were optimized. As a result, nine minima were located (three for each configuration of the amino acid fragment). The geometries of all the minima were subsequently reoptimized at the DFT/B3LYP/6-31++G** level. This was followed by harmonic frequency calculations at the same level of theory. MP2/6-31++G** single-point calculations were also performed at the DFT/B3LYP/6-31++G** optimal geometries. All calculations in this work were done on IBM RS6000 workstations using the Gaussian 94[31] quantum-mechanical program.

TABLE 1: Energies (in au), Relative Stabilities (ΔE, in kJ mol^{-1}), Zero-Point Vibrational Energies (ZPVE,[a] in au) and Relative Stabilities Including the ZPVE (ΔE_{Total}, in kJ mol^{-1}) of the Valine Conformers[a]

	DFT/B3LYP				MP2		
	energy	ΔE	ZPVE	ΔE_{Total}	energy	ΔE	ΔE_{Total}[b]
Ia	−402.410 022 5	0.00	0.158 599 9	0.00	−401.227 604 4	0.00	0.00
Ib	−402.409 470 7	1.45	0.158 714 9	1.75	−401.226 884 0	1.89	2.19
Ic	−402.408 344 9	4.41	0.158 788 3	4.90	−401.226 661 9	4.05	2.97
IIa	−402.410 705 1	−1.79	0.159 287 0	0.01	−401.226 808 6	2.07	3.89
IIb	−402.407 260 8	7.25	0.159 247 3	8.95	−401.222 808 6	12.59	14.29
IIc	−402.409 077 5	2.48	0.159 320 5	4.37	−401.226 481 1	2.95	4.84
IIIa	−402.407 974 7	5.38	0.158 777 7	5.84	−401.225 368 9	5.87	6.34
IIIb	−402.408 599 7	3.74	0.158 605 3	3.75	−401.226 257 8	3.53	3.55
IIIc	−402.406 900 6	8.20	0.158 828 8	8.80	−401.224 675 5	7.69	8.29

[a] IR frequency calculations performed at the DFT/B3LYP/6-31++G** level; MP2/6-31++G** single-point calculations done at the DFT/B3LYP/6-31++G** geometries. ZPVEs scaled with the scaling factors 0.95 for the OH, NH, and CH stretching vibrations and the scaling factor 0.98 for all other vibrations. [b] ZPVE from the DFT/B3LYP/6-31++G** calculation.

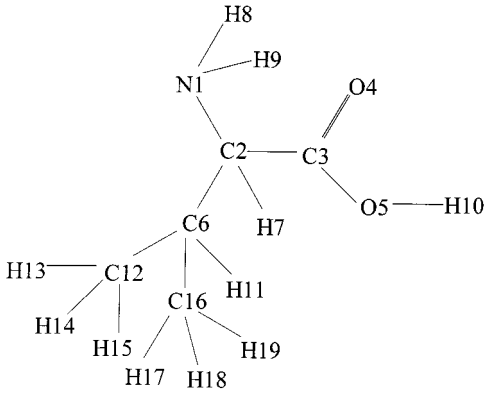

Figure 3. Atom numbering for valine.

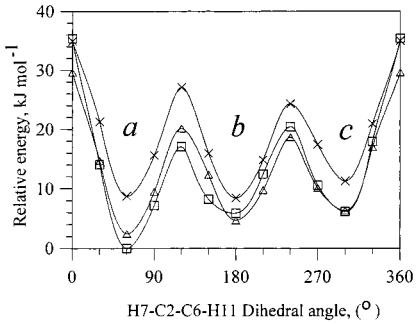

Figure 4. DFT/B3LYP/6-31G* energy vs H7−C2−C6−H11 dihedral angle. (△) conformer **I**, (□) conformer **II**, (×) conformer **III**.

4. Results and Discussion

Energies. The dependencies of the energy on the $H_7C_2C_6H_{11}$ dihedral angle (atom numbering is shown in Figure 3) in the valine conformers **I**−**III** are shown in Figure 4. As mentioned, three minima exists for each species. They are denoted as *a*, *b*, and *c*. The corresponding relative stability results are summarized in Table 1 and the structures of the conformers are shown in Figure 5. The DFT calculations predict the conformer **IIa** to be the global minimum, but the account of the zero-point vibrational energy (ZPVE) changes the stability order and conformer **Ia** becomes the most stable form. Its total energy is, however, only by 0.01 kJ mol^{-1} lower than the energy of conformer **IIa**. It should be noted that accounting for the ZPVE yielded a similar reversal of the stability order of the **I** and **II** glycine and alanine conformers.[8,13] This result indicates that for all amino acids studied the ZPVE contribution destabilizes the conformers with the N···H−O intramolecular H-bond with respect to the conformers with the bifurcated NH_2···O═C H-bond.

The single-point MP2 calculations also predict conformer **Ia** to be the global minimum with a more significant energy difference with respect to the other conformers (Table 1). In our studies on glycine and alanine we demonstrated that the conformers with relative energies within 6−7 kJ mol^{-1} to the most stable form may be present in low-temperature matrixes.[8,13] The data presented in Table 1 show that the relative energies of at least seven valine conformers, i.e., **Ia**, **Ib**, **Ic**, **IIa**, **IIc**, **IIIa**, and **IIIb**, fall within this limit and a possibility of their presence in the matrix should be considered.

Rotational Constants and Geometries. The rotational constants and dipole moments of the valine conformers calculated at the DFT/B3LYP/6-31++G** level of theory are presented in Table 2. Since the DFT-predicted rotational constants of the glycine and alanine conformers were very accurate (mean difference between the calculated and the experimental rotational constants was less than 1%),[8,13] it is reasonable to expect that the calculated rotational constants of the valine conformers are also predicted with a similar accuracy. Since, as mentioned, there has been no experimental attempt to determine microwave spectra of valine, the calculated rotational constants presented in Table 2 may be useful in searching for gas-phase valine conformers with the microwave spectroscopy. In this search the conformers with the N···H−O H-bonds (i.e., **IIa**−**c**) should give the strongest signals due to their higher dipole moments than the other low energy conformers.

Selected structural parameters of the lowest energy valine conformers **Ia** and **IIa** are presented in Table 3. These data may assist an analysis of electron-diffraction spectra of gaseous valine which has not yet been obtained. A comparison of the calculated geometrical parameters of the amino and carboxylic groups of glycine,[8] alanine,[13] and valine (Table 3) shows that, as expected, changes in the amino acid side chain do not significantly affect the bond lengths and bond angels of the amino acid fragment. The differences are within 0.01 Å and 3° for the bond lengths and bond angels, respectively.

IR Spectra. The assignment of the experimental matrix IR spectrum of valine is given in Table 4. The calculated IR frequencies and intensities of the valine conformers **Ia** and **IIa** are also presented in Table 4. The frequencies and intensities of other conformers are summarized in Table 5.

Analysis of the high-frequency region of the spectrum (3600−3000 cm^{-1}) allows identification of the OH stretching vibration of two valine conformers. In this region the highest frequency band at 3561 cm^{-1} (Figure 1) is attributed to the valine conformer **Ia** and the down-shifted experimental band at 3183 cm^{-1} is attributed to conformer **IIa**. This assignment is based on a close match between the experimental and the calculated

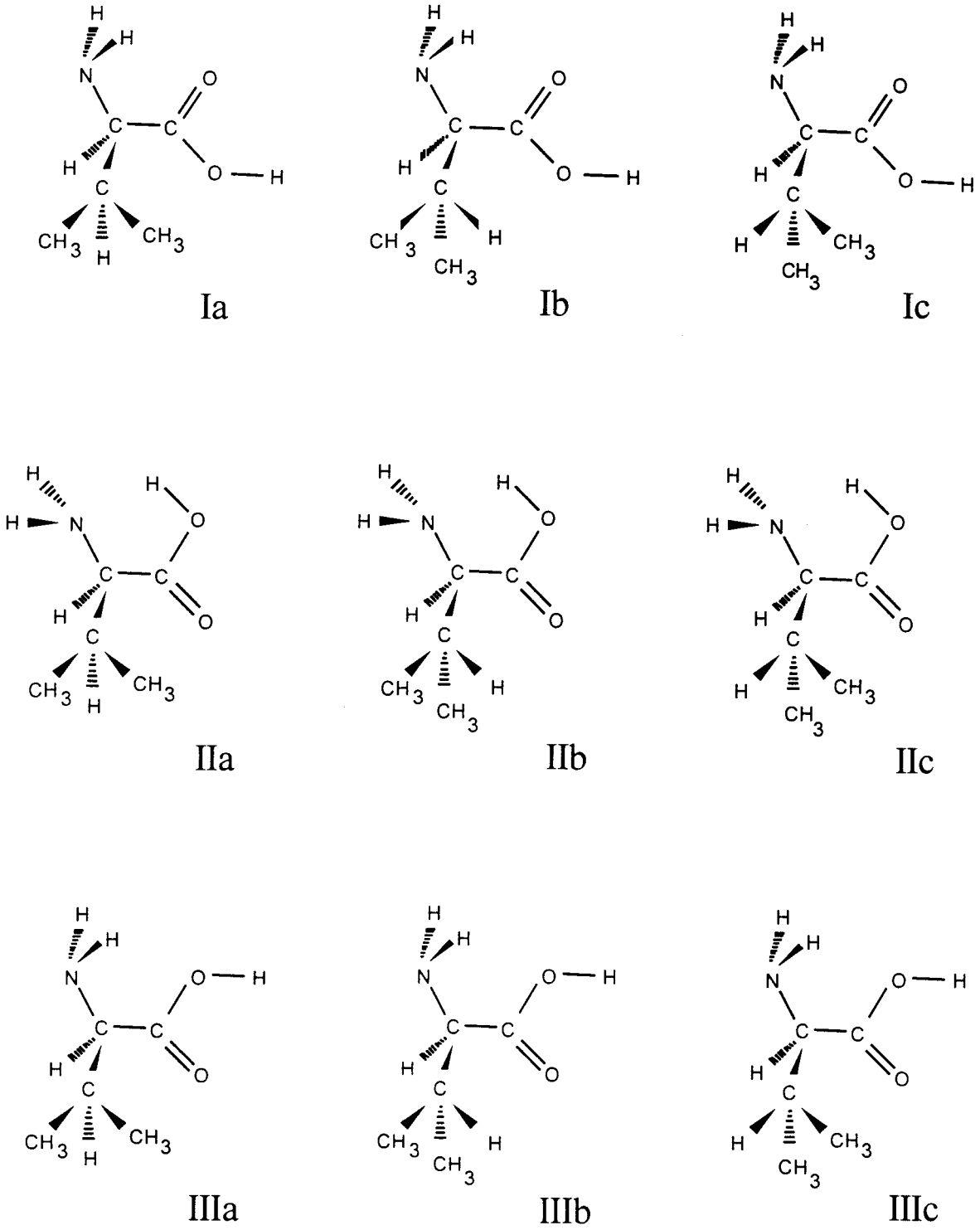

Figure 5. Structures of the valine conformers.

frequencies. The downward frequency shift of 378 cm^{-1} for the OH stretching vibration in conformer **IIa** is due to the intramolecular N···H−O H-bond. The H-bonding also causes a significant increase of the intensity of the OH stretch of the conformer **IIa** which helps to identify this band in the spectrum. The 378 cm^{-1} frequency shift in the valine **IIa** conformer is very similar to the shifts observed for glycine (360 cm^{-1})[8] and alanine (367 cm^{-1}).[13]

The predicted intensities of the NH stretching vibrations are much smaller than ones of the OH stretches. In the high-frequency region we only observe the band of the asymmetric NH_2 stretching vibration at 3422 cm^{-1} (see Table 4). The analysis of the high-frequency region confirms the presence of the valine conformers **Ia** and **IIa**, but the presence of conformers **IIIa**−**c** cannot be definitely confirmed since the calculations predict similar frequencies of the OH and NH stretches of these conformers and conformer **I** (see Tables 4 and 5).

Another region which provides information on the valine conformational composition is the region of the C═O stretching vibrations (1800−1700 cm^{-1}, see Figure 1). The most intensive band in this region at 1761 cm^{-1} is attributed to the lowest energy conformer **Ia**. The calulations predict a higher frequency shift of the C═O stretch for conformer **IIa** than that for conformer **Ia**. This allows us to assign the experimental band

TABLE 2: Rotational Constants (MHz) and Dipole Moments (Debye) of the Valine Conformers

	A_c	B_c	C_c	μ
Ia	2910	1410	1309	1.36
Ib	2791	1544	1213	1.30
Ic	2366	1746	1400	1.41
IIa	3007	1449	1240	5.54
IIb	2965	1573	1087	5.45
IIc	2465	1749	1401	5.46
IIIa	2961	1404	1295	1.60
IIIb	2823	1517	1232	1.66
IIIc	2388	1728	1410	1.53

[a] Quantities obtained in the DFT/B3LYP/6-31++G** calculations.

TABLE 3: Optimized Geometry Parameters of Valine Conformers Ia and IIa Obtained in the DFT/B3LYP/6-31++G Calculations**

bond lengths (Å)			bond angles (deg)			torsion angles (deg)		
	Ia	**IIa**		**Ia**	**IIa**		**Ia**	**IIa**
1-2	1.457	1.476	1-2-3	112.8	109.0	1-2-3-4	16.7	171.5
2-3	1.531	1.548	2-3-4	125.5	123.0	1-2-3-5	196.0	−10.4
3-4	1.214	1.211	2-3-5	112.3	114.1	4-3-2-6	250.9	219.6
3-5	1.357	1.342	3-2-6	110.2	111.4	4-3-2-7	135.4	103.7
2-6	1.561	1.548	3-2-7	106.6	104.3	3-2-1-8	73.5	261.6
2-7	1.096	1.098	2-1-8	110.6	112.0	3-2-1-9	−43.6	140.1
1-8	1.016	1.017	2-1-9	110.2	112.3	2-3-5-10	181.4	1.8
1-9	1.017	1.014	3-5-10	107.3	105.0	7-2-6-11	64.9	63.4
5-10	0.973	0.988	2-6-11	106.3	105.1	7-2-6-12	183.1	180.1
6-11	1.097	1.096	2-6-12	112.2	112.6	2-6-12-13	65.3	65.8
6-12	1.537	1.537	6-12-13	111.0	112.3	2-6-12-14	184.1	184.4
12-13	1.096	1.098	6-12-14	110.1	110.1	2-6-12-15	−56.0	−56.1
12-14	1.095	1.095	6-12-15	112.3	111.7	7-2-6-16	307.7	306.1
12-15	1.096	1.095	2-6-16	110.2	111.2	2-6-16-17	178.9	175.8
6-16	1.535	1.535	6-16-17	110.4	110.6	2-6-16-18	299.0	295.2
16-17	1.095	1.095	6-16-18	110.7	111.7	2-6-16-19	59.2	56.1
16-18	1.094	1.097	6-16-19	111.3	111.5			
16-19	1.096	1.096						

at 1784 cm^{-1} to the C═O stretching vibration of conformer **IIa**. The observed difference of 23 cm^{-1} between the C═O frequencies of the valine conformers **Ia** and **IIa** is in a good agreement with the calculated value of 30 cm^{-1}. Again, the difference is due to the N−H···O═C H-bond in the conformer **Ia**.

As it is seen from Figure 1, a minor band at 1770 cm^{-1} is observed in the region of the C═O stretching vibration. It could be assigned to the C═O stretching vibration of the conformer **IIIb**, which is the most preferable form among conformers **IIIa**−**c** (Table 1). This assignment would be in agreement with the calculated data (Table 5), but we must take into account that the band at 1770 cm^{-1} can be also attributed to a Fermi resonance or a site splitting which are often observed in the region of the C═O stretching vibrations. Therefore, to confirm the presence of conformer **IIIb** in the matrix, other vibrations need to be examined, particularly those with more significant predicted intensities. According to the calculation, the vibrations of conformer **IIIb** with the following predicted wavenumbers fall into this category: 1632, 1307, 1152, 878, 824, 794, 617, and 589 cm^{-1}. Some of these frequencies are identical or very close to the frequencies of the major conformer **Ia** and cannot serve as an evidence of the presence of conformer **IIIb** in the matrix. However there is a set of experimental bands at frequencies 1156, 882, 791, 625, and 580 cm^{-1} (see Table 4) which cannot be assigned to conformers **Ia** and **IIa**. These bands prove the presence of a trace amount of the **IIIb** valine conformer in the matrix.

In the region below 1500 cm^{-1} most of the experimental bands are assigned to the lowest energy conformer **Ia**. Some characteristic bands of conformer **IIa** are also observed. They are the bands of the OH bending vibrations at 1388, 1382 cm^{-1}, the NH_2 bending vibration at 975 cm^{-1}, the OH torsion vibrations at 877 and 825 cm^{-1}, and the C_2-C_6 stretching vibration at 783 cm^{-1}. As it is seen from Table 4, a few weak bands in the region below 1500 cm^{-1} are not assigned to conformers **Ia**, **IIa**, or **IIIb**. Some of these bands (marked in Table 4 with asterisks) may correspond to other valine conformers, but they can also be attributed to overtones or combination bands which are frequently present in the matrix IR spectra. Therefore we cannot definitely affirm or disproof the presence in the matrix of some trace amounts of other valine conformers.

In conclusion, the analysis of the matrix IR spectrum of valine allowed a definite identification of bands corresponding to three valine conformers **Ia**, **IIa**, and **IIIb**. By comparing the calculated and the observed intensities of the conformers, we estimated the conformational composition of the valine deposit in the Ar matrix. This estimated composition is the following: approximately 94% of conformer **Ia**, 5% of conformer **IIa**, and a trace amount (less than 2%) of conformer **IIIb**. It also should be noted that the MP2 relative energies of the valine conformers **Ia** and **IIa** better correlate with the experimental results than the DFT/B3LYP energies.

5. IR Spectral Characterization of the Amino Acid Conformers

Information presented in this work, as well as the results of our recent studies of other nonionized aliphatic amino acids,[8,13] allows identification of common IR spectral characteristics of these systems. These common features will be useful in future IR spectral investigations of other gas-phase amino acids and oligopeptides.

First, it should be noted that the most pronounced spectral differences between different amino acid conformers are due to the different intramolecular H-bonding interactions in these systems. For each of the amino acids studied three conformers were experimentally identified, i.e., the conformer with the NH_2···O═C H-bond, the conformer with N···H−O H-bond, and the conformer with the NH_2···O−C H-bond. The most significant differences in the IR vibrations of these conformers appear in the groups involved in the H-bonding, i.e., in the OH, NH, C═O and C−O groups.

The conformer with the NH_2···O═C H-bond is the global minimum for all the amino acids studied. An identification of this form in the IR spectrum is usually straightforward. The intensive bands of the OH stretches in the 3565−3555 cm^{-1} region, the bands of the C═O stretches in the 1790−1760 cm^{-1} region, the bands of the mixed CN and C−O stretching vibrations in the 1140−1100 cm^{-1} region, the NH_2 bending vibrations in the 890−870 cm^{-1} region, and the OH torsion vibrations in the 600−590 cm^{-1} region are the most important evidences of this lowest energy conformer, which is usually denoted as **I**. The characteristic vibrations of the **I** conformer including the bands of deuterated isotopomers are presented in Table 6.

The second most stable form of all the amino acids studied by us so far is the conformer with the N···H−O H-bond (usually denoted as **II**). Only the DFT and correlated ab initio calculations are able to correctly predict the relative energy of this conformer with respect to conformer **I**.[8,17,18] The HF method significantly overestimates this relative energy.[17,18] The bands that facilitate identification of conformer **II** in the experimental spectrum are those of the OH stretching and bending vibrations which are observed near 3200 and 1390 cm^{-1}, respectively. The

TABLE 4: Observed and Calculated (at the DFT/B3LYP/6-31++G Level) IR Frequencies (cm^{-1}) and Intensities of Valine**

observed[a]			calculated				
			valine **Ia**		valine **IIa**		
ν	A[b]	I_{obs}[c]	ν[d]	I_{calc}[e]	ν	I_{calc}[e]	PED[f]
3561	0.112	2.317	3558	57.5			OH str [100]
3549	0.081						
3537	0.051						
3422	0.016	0.681	3414	6.5	3437	13.9	NH_2 str asym [97]
3395	0.021						
			3338	1.8	3349	0.4	NH_2 str sym [96]
3183	0.025	0.589			3267	274.5	OH str [97]
2989	0.051	9.467					
2968	0.145		2969	24.4	2963	21.5	$C16H_3$ str [95]
			2953	22.0	2951	35.7	$C12H_3$ str [98]
			2950	35.3	2943	45.1	$C12H_3$ str [89]
2937	0.100		2943	32.2	2936	14.3	$C16H_3$ str [81]
2913	0.068		2910	15.0	2914	0.8	C2H str [88]
2897	0.057		2893	10.4	2895	8.9	C6H str [79]
2877	0.066		2886	15.8	2878	29.5	$C16H_3$ str [50], $C12H_3$ str [45]
2856	0.036		2882	41.5	2874	29.4	$C12H_3$ str [64], $C16H_3$ str [30]
1784	0.116	6.198			1799	309.9	C═O str [88]
1770	0.238						
1761	0.430		1769	292.7			C═O str [83]
1627	0.073	0.083	1643	35.5	1626	34.4	HNH bend [91]
			1489	7.8	1487	12.0	HC16H bend [73], HC12H bend [12]
1471	0.051	0.523	1480	9.3	1483	8.3	HC12H bend [75], HC16H bend [12]
1465	0.051		1471	2.8	1474	3.5	HC12H bend [52], HC16H bend [24]
			1461	1.3	1462	0.2	HC16H bend [49], HC12H bend [27]
			1401	11.2	1405	5.5	C2H bend [46], C6H bend [25]
1388	0.086	4.610			1386	190.1	OH bend [71], $C16H_3$ bend [18]
			1388	0.7			C2H bend [45], C6H bend [20]
1382	0.094				1384	256.5	OH bend [66], C−O str [22]
1374	0.097						
1367	0.087						
1361	0.069		1377	8.6	1371	7.7	$C16H_3$ bend [51], $C12H_3$ bend [27]
1356	0.083						
1342	0.045		1344	4.6			$C16H_3$ bend [39], $C12H_3$ bend [29]
1318	0.040		1337	3.5	1339	1.4	C2H bend [42], C2C6 str [18], OH bend [14]
1307	0.038		1307	32.5	1325	0.3	C6H bend [36], OH bend [24]
			1247	0.4	1256	0.6	$C16H_3$ bend [27], $C12H_3$ bend [21], OH bend [20]
			1210	0.4	1194	15.3	NH_2 bend [37], CN str [14], OH bend [14], $C12H_3$ bend [11]
			1183	0.4	1179	3.4	C6H bend [26], CN str [17], C2H bend [12]
1168	0.040	0.256		9.5	1173	12.0	C6H bend [31], CN str [15]
1156	0.047	0.310	1152[g]	122.4			C−O str [37], CN str [17], OH bend [15]
1136	0.049	0.141	1142	5.9	1137	2.7	CN str [32], C2C3 str [19], C3C2C6 bend [11]
1115	0.278	1.355					
1108	0.506	1.840	1114	254.0			C−O str [45], OH bend [26], CN str [14]
1101	0.094	0.443					
1050	0.068	0.235	1071	9.6	1061	6.8	$C16H_3$ bend [31], $C12H_3$ bend [19], CN str [17], C2H bend [13]
1044	0.027	0.077	1049	18.3	1015	8.4	$C12H_3$ bend [25], $C16H_3$ bend [21], C12C16 str [14]
975	0.042	0.211			975	61.2	NH_2 bend [38], C2C3str [29]
970	0.029						
962	0.027	0.112	953	7.2	949	2.2	C6C12 str[24], C6H bend [18]
949	0.023	0.062					
945	0.031	0.077	936	16.5			CN str [37], C6C12 str [17], C6C16 str [13]
937	0.018	0.068					
921	0.035	0.102	919	7.5	919	1.9	C6C16 str [19], C6C12 str [14]
890	0.073	1.110	887	46.6	888	68.9	NH_2 bend [69], CN str [19]
882	0.050		878[g]	46.7			NH_2 bend [64]
877	0.073				867	77.4	OH tor [64]
836	0.056	0.259	834*	69.6			
825	0.121	3.580			823	56.8	OH tor [37], NH_2 bend [21]
817	0.304		821	14.2			NH_2 bend [21],C2C3 str [20], CN str [15]
806	0.208		813	6.2			C6C12 str [35], NH_2 bend [19]
800	0.083		812*	61.0			
791	0.081	0.413	794[g]	78.7			C6C12 str [31], NH_2 bend [16]
783	0.111	0.773			792	22.2	C2C6 str [24], C═O bend [18]
741	0.033	0.073	740*	40.6			
721	0.028	0.109	714*	38.4	712	8.0	C2C6 str [29], C2C3 str [15], C−O str [10]
706	0.044	0.243	695	31.8			C2C6 str [31], C2C3 str [12]
704	0.062						

TABLE 4 (Continued)

observed[a]			calculated				
			valine **Ia**		valine **IIa**		
ν	A[b]	I_{obs}[c]	ν[d]	I_{calc}[e]	ν	I_{calc}[e]	PED[f]
655	0.024	0.072	654*	18.0			C═O bend [37], C3C2C6 bend [17], NC2C3 bend [15]
645	0.022	0.120	645*	22.1			C═O bend [42], NC2C3 bend [19], C2C6C12 bend [10]
634	0.034	0.514	640	34.8			C═O bend [43], NC2C3 bend [21]
629	0.048						
625	0.087		617[g]	48.2			OH tor [84]
600	0.040	0.150	613*	88.4			
595	0.118	0.620	608	85.8			
593	0.139						
588	0.142	0.518	596	44.8	593	9.2	OH tor [88]
584	0.056						
580	0.036	0.133	589[g]	93.2			OH tor [49], C2C3-O bend [21]
572	0.034	0.072					
564	0.079	0.188					
551	0.036	0.428	559	36.8			C2C3-O bend [48], C3C2C6 bend [13]
548	0.106						
541	0.075	0.227					
522	0.028	0.130	511*	13.9			
517	0.033	0.054	508*	16.6	506	2.1	C2C3-O bend [39], C3C2C6 bend [10]
			428	17.9			C2C3 tor [27], C2C3-O bend [17], OH tor [11]
			385	1.4	403	1.6	NC2C3 bend [25], C2-C3 tor [13]
			334	8.7	355	9.2	C3C2═O bend [27], C2-C3 tor [15]
					302	7.0	NC2C3 bend [31], NH_2 tor [17], C2C6 tor [10]
			283	6.8	288	12.9	NC2C3 bend [38], NH_2 tor [21]
			250	6.1	265	4.4	C3C2C6 bend [47], NC2C3 bend [11]
			246	1.1	248	0.4	C6C12 tor [29], C6C16 tor [21]
			213	1.3	225	0.7	C6C16 tor [32], C6C12 tor [18]
			188	38.2			NH_2 tor [87]
			169	0.0	177	8.1	C3C2C6 bend [70]
			74	0.4	83	3.5	C2C6 tor [67]
			50	1.1	56	0.6	C2C3 tor [49]

[a] Ar matrix deposited at 14 K. Sample-to-matrix ratio 1:1000. [b] A, experimental relative intensities. [c] I_{obs}, experimental relative integral intensities measured for the single bands or for the groups of bands. [d] Frequencies marked with asterisks are taken from the calculated spectra of other low energies valine conformers which are presented in Table 5. [e] I_{calc}, calculated intensities in km mol^{-1}. [f] Potential energy distributions (PED) are given in square brackets. Only contributions ≥ 10% are listed. Abbreviations: str, stretching; bend, bending; tor, torsion, sym, symmetric; asym, asymmetric. [g] Bands assigned to the conformer **IIIb**.

N···H−O H-bonding elevates the intensities of these bands, which helps in their identification. Practically, the presence of a band at approximately 3200 cm^{-1} in the spectrum of a nonionized amino acid provides a sufficient proof of the presence of conformer **II**. The band corresponding to the C═O stretching vibration of conformer **II** is always upshifted with respect to the corresponding band of the conformer **I** by 20−30 cm^{-1} and has lower intensity. Other characteristic vibrations of conformer **II**, as well as the bands of its deuterated derivative, are summarized in Table 6.

As seen from Table 6, the spectral manifestations of the H-bonding are very different for the OH and NH_2 vibrations. The changes in frequencies of the OH stretching and bending vibrations upon the H-bonding are approximately 360 and 120 cm^{-1}, respectively. The corresponding changes of the NH_2 group vibrations are only 40 and 10 cm^{-1}, respectively. This difference provides a spectral evidence that the intramolecular N···H−O H-bond in amino acids is stronger than the NH_2···O═C H-bond.

The location of the third amino acid conformer with the NH_2···O−C H-bond (denoted as **III**) is more difficult for two reasons. First, usually a small amount of this conformer is present in the matrix and its bands are very weak. Second, the NH_2···O═C H-bond in the conformer **I** and NH_2···O−C H-bond in the conformer **III** have similar spectral manifestations. As a result, the frequency differences between the corresponding bands of these two conformers are within a few wavenumbers from each other for most vibrations. The most conclusive proof of the presence of conformer **III** is based on the analysis of the C═O stretching vibration region, since the C═O stretch is the most intensive vibration of this conformer. The position of the band due to the C═O stretch of the conformer **III** with respect to the one of the conformer **I** varies in the spectra of different amino acids. The calculated frequency is used here to make a positive identification because, as we demonstrated in this and previous studies, the predicted direction and the magnitude of the shift of the C═O stretching vibration agrees very well with the experiment. In the IR spectrum of alanine in the region of the C═O stretching vibrations only two bands were observed and they were assigned to conformers **I** and **II**. Therefore, we concluded that conformer **III** of alanine is not present in the matrix. However, for glycine and valine a third band appeared in the spectral region of the C═O vibrations in the position which agreed with the calculated frequency. This finding allowed us to postulate the presence of conformers **III** of glycine and valine in the matrixes. To confirm this presence further analysis of bands in other spectral regions was performed. The selection of these bands was made based on the calculations and included the most intensive vibrations of conformer **III**. The analysis was described in the previous section of this paper.

6. Conclusions

The conformational behavior of nonionized natural amino acid α-valine has been studied by means of the low-temperature

TABLE 5: Calculated DFT/B3LYP/6-31++G Harmonic Frequencies (cm^{-1}) and Intensities (km mol^{-1}) of the Valine Conformers[a]**

Ib		Ic		IIb		IIc		IIIa		IIIb		IIIc	
frequency	intensity	frequency	intensity	frequency	intensity	frequency	intensity	frequency	intensity	frequency	intensity	frequency	intensity
3545	52.2	3549	53.0	3428	8.9	3425	10.0	3561	66.3	3565	68.9	3563	67.0
3409	5.5	3410	5.7	3335	0.9	3344	0.9	3428	5.3	3420	5.2	3421	4.7
3324	1.3	3332	1.0	3268	280.8	3277	247.9	3350	1.6	3333	1.3	3341	0.8
2982	12.3	2961	31.1	3007	2.1	2977	13.6	2967	25.8	2980	13.7	2961	35.3
2955	34.7	2955	50.3	2955	35.5	2956	27.9	2950	34.3	2954	35.3	2952	37.5
2949	50.9	2952	38.9	2943	59.3	2954	29.8	2947	31.9	2949	49.9	2951	39.8
2939	19.9	2948	3.3	2936	15.5	2951	24.5	2945	27.1	2939	20.2	2949	10.8
2922	14.0	2923	13.2	2883	51.7	2897	21.9	2908	14.3	2928	9.8	2926	10.4
2885	31.1	2892	13.1	2877	15.0	2891	15.2	2900	3.1	2885	30.0	2892	10.2
2879	27.6	2889	15.2	2875	19.0	2887	29.4	2886	18.7	2879	27.9	2889	18.8
2867	6.4	2885	29.5	2860	3.5	2842	37.5	2881	38.4	2869	7.6	2884	30.0
1768	278.2	1767	278.1	1799	308.3	1798	301.9	1767	277.2	1772	319.7	1766	280.8
1634	37.5	1642	38.6	1630	30.7	1628	49.2	1643	42.5	1632	39.5	1641	43.6
1489	16.5	1486	15.3	1496	15.0	1487	12.8	1488	8.3	1488	12.6	1486	13.9
1480	3.9	1479	5.8	1479	6.6	1481	9.7	1482	9.5	1480	5.3	1480	6.1
1465	1.5	1469	1.7	1471	1.7	1468	4.1	1470	3.1	1465	1.0	1470	2.7
1462	4.9	1461	1.4	1462	5.7	1464	0.4	1461	1.2	1463	4.1	1461	0.2
1403	6.9	1406	7.7	1399	1.4	1408	11.6	1399	6.5	1400	8.9	1406	7.6
1386	13.1	1397	5.0	1383	452.1	1387	62.5	1378	7.2	1378	3.9	1387	7.9
1377	4.2	1385	9.6	1378	11.7	1385	276.7	1373	11.9	1371	5.8	1372	10.6
1345	14.8	1354	3.4	1360	4.3	1348	40.3	1343	1.1	1345	6.5	1353	10.3
1330	12.6	1321	12.3	1343	3.4	1343	18.2	1338	5.7	1323	0.4	1325	12.6
1315	15.9	1292	21.2	1310	0.5	1316	12.1	1313	38.6	1307	39.3	1302	25.3
1251	1.3	1252	1.5	1251	7.0	1274	8.0	1265	0.6	1281	6.8	1268	3.1
1218	6.7	1212	11.1	1183	4.4	1220	5.3	1202	14.6	1218	6.1	1209	8.9
1168	9.5	1178	1.7	1179	18.9	1182	3.6	1182	5.0	1167	6.1	1179	7.6
1126	96.8	1125	175.9	1161	12.0	1168	23.8	1148	140.9	1152	122.4	1153	131.0
1116	155.4	1114	63.6	1122	4.3	1101	1.6	1139	68.9	1107	47.4	1101	12.0
1087	14.9	1099	40.4	1084	16.0	1070	8.4	1068	17.0	1077	26.2	1094	86.8
1047	7.6	1063	3.1	1040	8.7	1054	11.6	1043	39.7	1045	11.3	1062	16.2
964	21.2	949	0.8	965	105.8	952	2.7	949	3.7	956	13.8	952	0.2
938	18.2	933	14.0	946	0.4	930	1.2	930	11.4	930	24.6	929	4.2
918	1.3	916	0.9	917	1.3	921	59.2	917	12.4	913	6.9	915	3.4
888	35.4	894	91.7	899	61.5	902	55.9	878	62.5	878	46.7	880	107.2
834	69.6	823	80.1	873	71.8	871	78.7	810	5.9	824	63.0	806	74.3
812	61.0	796	7.1	823	44.6	827	21.1	802	107.6	794	78.7	793	13.5
740	40.6	714	38.4	807	27.7	784	22.0	698	49.6	749	21.3	713	31.8
645	22.1	654	18.0	711	8.8	718	9.9	640	68.8	617	48.2	638	53.6
613	88.4	608	85.8	569	8.4	637	7.4	594	26.6	589	93.2	588	74.3
508	16.6	511	13.9	540	1.3	527	3.3	556	36.4	519	10.3	526	16.2
420	2.6	443	5.7	448	2.6	459	2.1	453	8.8	426	2.3	447	5.9
369	5.2	381	8.4	399	6.0	422	0.8	388	2.1	377	6.5	394	5.7
348	8.9	345	2.6	354	17.7	346	1.2	327	4.2	344	8.3	349	1.2
296	8.4	290	18.2	345	6.1	329	13.6	286	4.7	295	17.7	287	9.9
266	8.3	270	9.9	342	3.7	275	16.6	268	23.0	266	18.1	252	12.0
254	28.8	238	3.9	285	6.6	255	3.8	253	0.5	259	3.1	249	20.7
233	1.3	233	7.5	243	2.4	242	3.0	228	22.9	225	0.7	240	13.2
209	0.5	219	22.5	225	3.7	223	0.1	213	1.2	207	0.1	228	0.5
165	0.1	168	0.1	198	6.0	176	5.1	170	0.6	162	0.0	169	0.7
69	0.3	86	0.4	76	1.9	93	1.3	73	0.1	69	0.2	84	1.0
51	1.8	33	1.1	40	1.6	64	1.3	37	1.6	49	1.1	34	0.8

[a] Data for the valine conformers **Ia** and **IIa** are presented in Table 4 together with the experimental results.

TABLE 6: IR Spectral Regions (cm^{-1}) of the Characteristic Vibrations of the Nonionized Amino Acid Conformers I and II Isolated in Inert Gas Matrices

vibration	conformer **I**		conformer **II**	
	normal	deuterated[a]	normal	deuterated[a]
OH(D) stretching	3565−3555	2640−2620	3210−3180	2600−2570
$NH(D)_2$ stretching asymmetrical	3420−3410	2560−2540	3460−3440[b]	2600−2570[b]
C═O stretching	1790−1760	1780−1760	1810−1780	1800−1780
OH(D) bending+C−O stretching[c]	1290−1270	1290−1270	1400−1380	1290−1270
		1110−990		1000−990
$NH(D)_2$ bending	1645−1625	1230−1220	1625−1620	1220−1210
OH(D) torsion	650−600	470−430	870−820	630−610

[a] Deuterated at N and O atoms. [b] Based on calculated data. [c] Bands assigned to this mixed vibration in the IR spectra of deuterated compounds are observed in two regions.

matrix isolation IR spectroscopy and with DFT and ab initio calculations. Three valine conformers stabilized by intramolecular H-bonds were detected based on the analysis of the experimental IR spectra assisted by comparison with the

calculated IR frequencies and intensities. The conformational composition of valine was estimated as ∼94% of conformer **Ia**, ∼5% of conformer **IIa**, and a trace amount (<2%) of conformer **IIIb**. The structure and relative energies of nine lowest-energy valine conformers were calculated at the DFT/B3LYP/6-31++G** and MP2/6-31++G** levels of theory. The calculations predicted the conformer **Ia** to be the global minimum on the valine potential energy surface. This is in agreement with the experimental data. The structural parameters of the valine conformers (geometries, rotational constants, and dipole moments) predicted in this work can be useful in a search for gas-phase valine conformers using the microwave spectroscopy and electron-diffraction methods.

An analysis of the spectral features corresponding to different valine conformers and their comparison to the spectra of glycine and alanine have allowed identification of common spectral characteristics of the structurally similar amino acid conformers. These common features will guide future studies of conformational behavior of larger amino acids, as well as those of small peptides.

Acknowledgment. This work was supported in part by a NATO grant (CRG.CRG 973389) allowing the visit of Dr. S. Stepanian to the University of Arizona.

References and Notes

(1) Brown, R. D.; Godfrey, P. D.; Storey, J. W. V.; Bassez, M. P. *J. Chem. Soc., Chem. Commun.* **1978**, 547.

(2) Suenram, R. D.; Lovas, F. J. *J. Mol. Spectrosc.* **1978**, *72*, 372.

(3) (a) Suenram, R. D.; Lovas, F. J. *J. Am. Chem. Soc.* **1980**, *102*, 7180. (b) Schäfer, L.; Sellers, H. L.; Lowas, F. J.; Suernam, R. D. *J. Am. Chem. Soc.* **1980**, *102*, 6566.

(4) Iijima, K.; Tanaka, K.; Onuma, S. *J. Mol. Struct.* **1991**, *246*, 257.

(5) Godfrey, P. D.; Brown, R. D. *J. Am. Chem. Soc.* **1995**, *117*, 2019.

(6) Lovas, F. J.; Kawashima, Y.; Grabow, J.-U.; Suenram, R. D.; Freser, G. T.; Hirota, E. *Astrophys. J.* **1995**, *455*, 201.

(7) Reva, I. D.; Plokhotnichenko, A. M.; Stepanian, S. G.; Ivanov, A. Yu.; Radchenko, E. D.; Sheina, G. G.; Blagoi, Yu. P. *Chem. Phys. Lett.* **1995**, *232*, 141. Erratum. *Chem. Phys. Lett.* **1995**, *235*, 617.

(8) Stepanian, S. G.; Reva, I. D.; Rosado, M. T. S.; Duarte, M. L. T. S.; Fausto, R.; Radchenko, E. D.; Adamowicz, L. *J. Phys. Chem.* **1998**, *102A*, 1041.

(9) Iijima, K.; Beagley, B. *J. Mol. Struct.* **1991**, *248*, 133.

(10) Godfrey, P. D.; Firth, S.; Hatherley, L. D.; Brown, R. D.; Pierlot, A. P. *J. Am. Chem. Soc.* **1993**, *115*, 9687.

(11) Debies, T. P.; Rabalais, J. W. *J. Electron Spectrosc. Relat. Phenom.* **1974**, *3*, 315.

(12) Klasinc, L. *J. Electron Spectrosc. Relat. Phenom.* **1976**, *8*, 161.

(13) Stepanian, S. G.; Reva, I. D.; Radchenko, E. D.; Adamowicz, L. *J. Phys. Chem.* **1998**, *102A*, 4623.

(14) Reva, I. D., Stepanian, S. G.; Plokhotnichenko, A. M.; Radchenko, E. D.; Sheina, G. G.; Blagoi, Yu. P *J. Mol. Struct.* **1994**, *318*, 1.

(15) Yu, D.; Rauk, A.; Armstrong, D. A. *J. Am. Chem. Soc.* **1995**, *117*, 1789.

(16) Barone, V.; Adamo, C.; Lelj, F. *J. Chem. Phys.* **1995**, *102*, 364.

(17) Császár, A. *J. Mol. Struct.* **1995**, *346*, 141.

(18) Császár, A. *J. Am. Chem. Soc.* **1992**, *114*, 9568.

(19) Frey, R. F.; Coffin, J.; Newton, S. Q.; Ramek, M.; Cheng, V. K. W.; Momany, F. A.; Schäfer, L. *J. Am. Chem. Soc.* **1992**, *114*, 5369.

(20) Császár, A. G. *J. Phys. Chem.* **1996**, *100*, 3541.

(21) Cao, M.; Newton, S. Q.; Pranata, J.; Schäfer, L. *J. Mol. Struct. (THEOCHEM)* **1995**, *332*, 251.

(22) Gronert, S.; O'Hair, A. J. *J. Am. Chem. Soc.* **1995**, *117*, 2071.

(23) Schäfer, L.; Kulp-Newton, S. Q.; Siam, K.; Klimkowski, V. J.; Van Alsenoy, C. *J. Mol. Struct. (THEOCHEM)* **1990**, *209*, 373.

(24) Shirazian, S.; Gronert, S. *J. Mol. Struct. (THEOCHEM)* **1997**, *397*, 107.

(25) Radchenko, E. D., Sheina, G. G.; Smorygo N. A.; Blagoi Yu. P. *J. Mol. Struct.* **1984**, *116*, 387.

(26) Binkley, J. S.; Pople, J. A. *Int. J. Quantum Chem.* **1975**, *9*, 229.

(27) Pople, J. A.; Binkley, J. S.; Seeger, R. *Int. J. Quantum Chem., Quantum. Chem. Symp.* **1976**, *10*, 1.

(28) Becke, A. D. *Phys. Rev. B* **1988**, *38*, 3098.

(29) Lee, C.; Yang, W.; Parr, R. G. *Phys. Rev. B* **1988**, *37*, 785.

(30) Vosko, S. H.; Wilk, L.; Nusair, M. *Can. J. Phys.* **1980**, *58*, 1200.

(31) Frisch, M. J.; Trucks, G. W.; Schlegel, H. B.; Gill, P. M. W.; Johnson, B. G.; Robb, M. A.; Cheeseman, J. R.; Keith, T.; Petersson, G. A.; Montgomery, J. A.; Raghavachari, K.; Al-Laham, M. A.; Zakrzewski, V, G.; Ortiz, J. V.; Foresman, J. B.; Cioslowski, J.; Stefanov, B. B.; Nanayakkara, A.; Challacombe, M.; Peng, C. Y.; Ayala, P. Y.; Chen, W.; Wong, M. W.; Andres, J. L.; Replogle, E. S.; Gomperts, R.; Martin, R. L.; Fox, D. J.; Binkley, J. S.; Defrees, D. J.; Baker, J.; Stewart, J. P.; Head-Gordon, M.; Gonzalez, C.; Pople, J. A. *Gaussian 94, Revision E.2*; Gaussian Inc.: Pittsburgh, PA, 1994.